BULLETIN OF THE EARTHQUAKE
RESEARCH INSTITUTE
Vol. 48 (1970), pp. 691-706

37. *Dispersion of Surface Waves in High-Velocity Layer Models.*

By Toshikatsu YOSHII,
Earthquake Research Institute.

(Read June 23, 1970.—Received July 15, 1970.)

Abstract

The models investigated here consist of a superficial or a sandwiched high-velocity layer and a lower-velocity half space medium. The idea of the so-called leaking mode plays an important role in understanding the dispersive character of these models.

Approximate dispersion curves of leaking modes have been calculated for various high-velocity layer models by the present author. The results are somewhat unusual; for example, a part of the phase velocity curves for these models often shows an inverse dispersion. This feature suggests a strong resemblance to the M_{21} wave in a simple "plate" model.

Model experiments were done to examine the reliability of the approximate dispersion curves. The agreement of the observed data with those curves is satisfactory.

Complex roots of the period equations are also calculated for the same models. Phase velocity curves derived from real parts of them agree well with the approximate ones. Imaginary parts of the complex roots give the attenuation of the leaking modes. Attenuation coefficients observed in a model experiment were well explained by the imaginary part.

The idea of the leaking mode seems to be the most easy and beautiful approach to understanding the dispersive feature of the high-velocity layer models.

1. Introduction

It is a very interesting problem to study the dispersion of surface waves propagating in a model with a superficial or a sandwiched high-velocity layer and a low-velocity half space. Such a model is called simply a "high-velocity layer model" in the present study. In understanding the dispersive feature of the models studied, the so-called leaking mode plays an important role because the phase velocity of the surface wave is often greater than the shear wave velocity in the half space.

The concept of the leaking mode arises from the residues of the

complex poles in the integral of the wave form [Rosenbaum (1960)]. Phinney (1961) and Gilbert (1964) calculated the complex roots of the period equations and discussed the dispersion of leaking modes. Phase velocity and attenuation of the leaking mode can be derived from the real and the imaginary parts of the complex root, respectively.

In contrast to this complex root method, Oliver and Major (1960) and Su and Dorman (1964) proposed simple approximate methods. Though they arrived at those methods rather intuitively, Tazime and Yoshii (1969) theoretically confirmed their validity. Approximate dispersion curves of the leaking modes for several high-velocity layer models have been investigated by the present author [Yoshii (1969), Yoshii and Suzuki (1969)].

The present study mainly consists of the following three parts:

1) Summary of the approximate dispersion curves.
2) Discussions on the resemblance between dispersive features of the high-velocity layer models and of the so-called plate models.
3) Comparison between dispersion curves derived from complex roots and from the approximate solutions.

These discussions will clarify the characteristics of the leaking modes in the high-velocity layer models.

2. Approximate dispersion curves of leaking modes in high-velocity layer models

Some of the approximate dispersion curves for various high-velocity layer models are summarized in this section. The leaking modes analyzed are those of Rayleigh type.

Five high-velocity layer models of the sandwiched type are schematically illustrated in Fig. 1. They are simply called "PAL-models" because they consist of plastics, aluminum and Lamiverre plates which were prepared as constituent media for the model experiment. The elastic constants of these plates are tabulated in Table 1. H_2/H_1 values of PAL-02, PAL-05, PAL-1, PAL-2, PAL-5 are 0.2, 0.5, 1.0, 2.0 and 5.0 res-

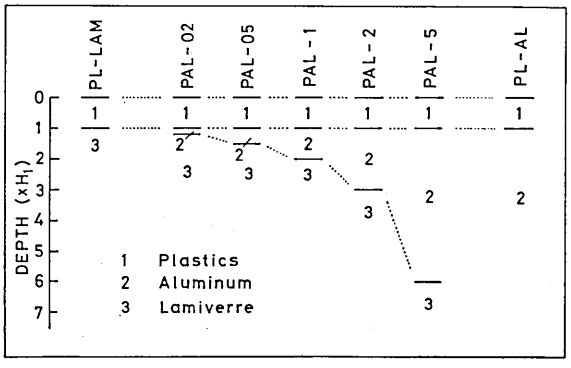

Fig. 1. Schematic representation of five PAL-models, the PL-LAM model and the PL-AL model.

Table 1. Elastic constants of the constituent media.

Medium	α	β	ρ
Aluminum	5.35	3.06	2.70
Lamiverre	3.45	1.55	1.75
Plastics	1.89	1.07	1.40

α=compressional wave velocity (km/s)
β=shear wave velocity (km/s)
ρ=density (gm/cm^3)

pectively. H_i indicates the thickness of the ith layer. The limits of $H_2/H_1 \to 0$ and $H_2/H_1 \to \infty$ correspond to Plastics-Lamiverre (PL-LAM) and Plastics-Aluminum (PL-AL) models respectively. It is noticeable that they both are usual models of a low-velocity layer overlying a half space type.

It is easily expected that the dispersive character of a PAL-model with a large H_2/H_1 value should be very similar to that of the PL-AL model especially in the higher-frequency range. This suggests that a part of surface waves in the PAL-models may be the leaking modes because normal modes for the PL-AL model have phase velocities higher than the shear wave velocity β_3 in the half space of the PAL-models.

An example of the calculation by the approximate methods [Oliver and Major (1960), Su and Dorman (1964)] is shown in Fig. 2. The model is PAL-2 and the phase velocity is 1.60 km/s. The uppermost figure shows the absolute value of Δ and the lower two figures show the spectra of the surface motion due to an incident S wave from the half space [Haskell (1962)]. The minima of $|\Delta|$ and the maxima of the spectra agree with each other very well. Approximate dispersion curves of the leaking modes were obtained by tracing these extremes.

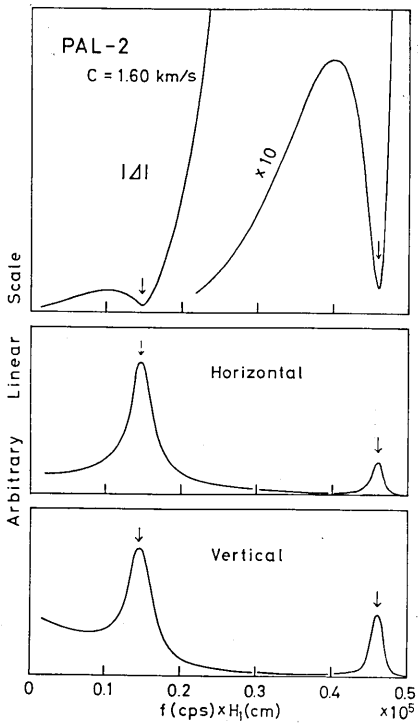

Fig. 2. Examples of calculations by two approximate methods for PAL-2. Upper: Oliver and Major's method. Middle and Lower: Su and Dorman's method.

The dispersion curves thus obtained are given in Fig. 3. Solid and

dashed lines indicate the normal and leaking modes, respectively. In this figure, dispersion curves of normal modes for the PL-LAM and PL-AL models are shown by chain lines for reference.

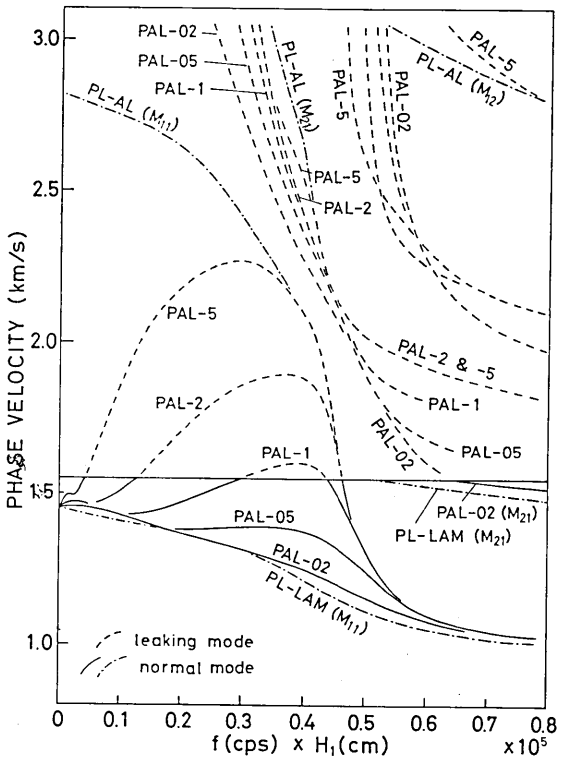

Fig. 3. Phase velocity curves for PAL-models, the PL-LAM model and the PL-AL model. Dashed lines indicate the approximate dispersion curves of leaking modes. The abscissa is the frequency multiplied by H_1.

The behaviour of the "fundamental modes" for the PAL-models are very interesting. That is, as the H_2/H_1 value increases, the phase velocity curve of this mode swells upward with its maximum increasing, and approaches that of the M_{11} wave for the PL-AL model which has no maxima. The PAL-model with a large H_2/H_1 value is almost equivalent to the PL-AL model in the higher frequency range as far as the dispersive feature is concerned. The second layer in such a model may behave like a half space for the wave whose wave length is approximately shorter than (H_1+H_2). Very complicated curves in the lower frequency range will be clearly shown in the next figure.

Although Fig. 3 gives only an example for models with a special velocity contrast, the dispersive features of any other sandwiched high-velocity layer model may be similar to those presented here.

In Fig. 4, the dispersion curves of the "fundamental mode" for the same models as in Fig. 3 are shown with the frequency multiplied by H_2 as the abscissa. In this case, the limit of H_2/H_1 tending to infinity corresponds to that of H_1 approaching zero, because H_2 is now assumed to be a finite value. It is soon realized that a model without the first layer is the AL-LAM model. This simple model consists of a superficial high-velocity layer and a low-velocity half space. As shown in Fig. 4, the dispersion curve for the AL-LAM model is characterized by the leaking mode shown with a dashed line. The existance of an "inverse

dispersion" suggests the resemblance between this wave and the M_{21} wave in the so-called plate model. The detailed discussion on this resemblance will be given in the section 3.

Two-dimensional model experiments were done to examine the reliability of this approximate dispersion curve for the AL-LAM model [Yoshii and Suzuki (1969)]. Three models with layer thicknesses of 0.4, 1.0 and 2.0 cm were prepared for the purpose of broadening the relative frequency range of the observation. Some of the records obtained from a model with the layer thickness of 1.0 cm are given in Fig. 5. The source signal applied to the free surface was a pulse of about 7 μs duration.

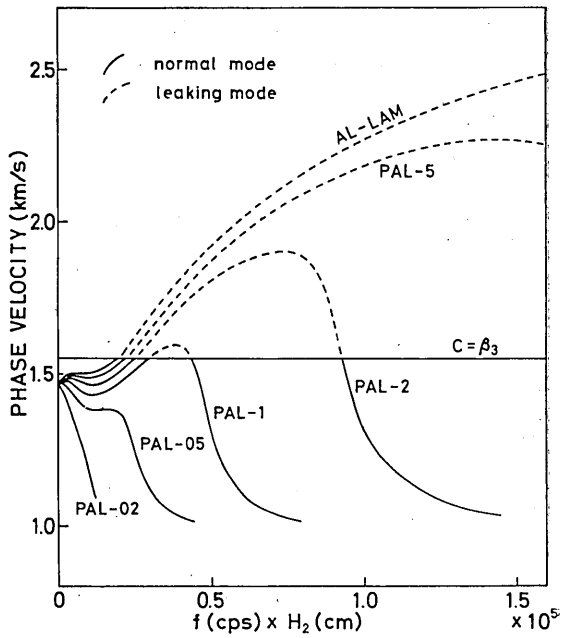

Fig. 4. Phase velocity curves for PAL-models and the AL-LAM model. The abscissa is the frequency multiplied by H_2.

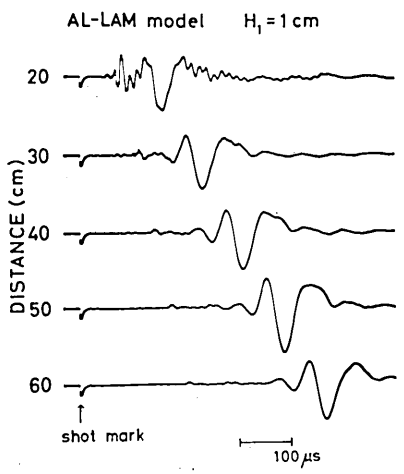

Fig. 5. Records obtained from model experiments for the AL-LAM model. The layer thickness is 1 cm.

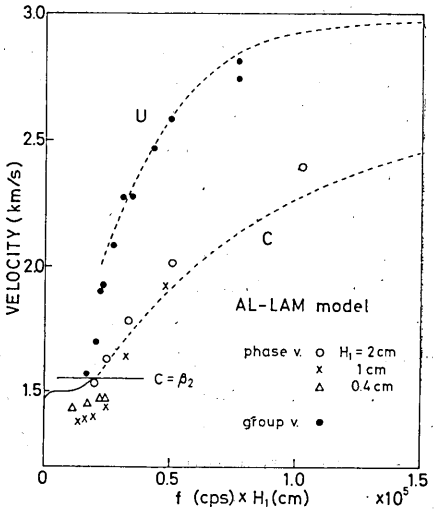

Fig. 6. Observed dispersion data and approximate dispersion curves for the AL-LAM model. The observed data were obtained by the usual peak and trough analysis.

These records are characterized by the inverse dispersion. It is also remarkable that the short period portion of the wave trains decays very rapidly. Observed phase and group velocity data from the peak and through analyses are given in Fig. 6. They agree well with the approximate dispersion curves except for small discrepancies in the lower frequency range. The discrepancies may arise from the observation error of the elastic constants, especially β_3, which were used in the theoretical calculations. A Lamiverre plate is not so good as the constituent medium because it is anisotropic.

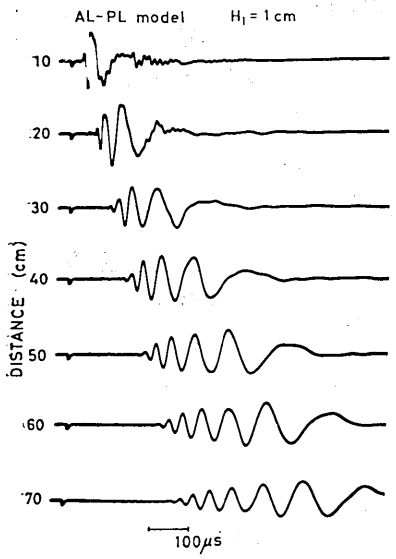

Fig. 7. Records obtained from model experiments for the AL-PL model. The layer thickness is 1 cm.

The AL-PL model is also a high-velocity layer model with the larger velocity contrast. Some of the records obtained with this model during the experiment are given in Fig. 7. The wave trains terminate their oscillatory movement suddenly like the Airy phase, while the M_{21} wave in the simple plate model continues infinitely due to zero group velocity. The agreement of the observed dispersion data with the approximate dispersion curves is satisfactory, as given in Fig. 8. The observed phase velocity data in this figure were derived by means of the Fourier analysis.

A similar model experiment has been done by Oliver, Press and Ewing (1954), but only the observed data were given by them because the idea of the leaking mode was not well known at that time.

Although the approximate dispersion curves for the high-velocity layer models have very peculiar forms, their reliability was, at least for the AL-LAM and AL-PL models, confirmed by the model experiments.

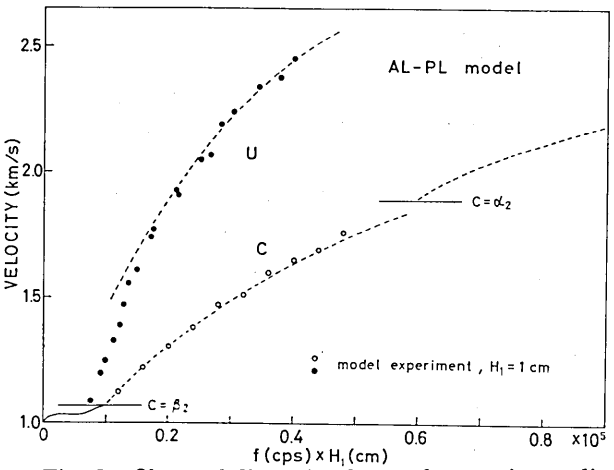

Fig. 8. Observed dispersion data and approximate dispersion curves for AL-PL model. Observed phase velocity data (open circles) were obtained by the Fourier analysis.

In general, a model experiment is a very useful tool to confirm especially an incomplete theory, because it may provide ideal observation data.

3. Resemblance of dispersive features between high-velocity layer models and simple plate models

It is obvious from Figs. 5 and 7 that these wave trains are very similar to the M_{21} wave, or the antisymmetric vibration, propagating in the "plate" model [e.g. Press and Oliver (1955)]. This resemblance is also indicated by an "inverse dispersion" in the phase velocity curves.

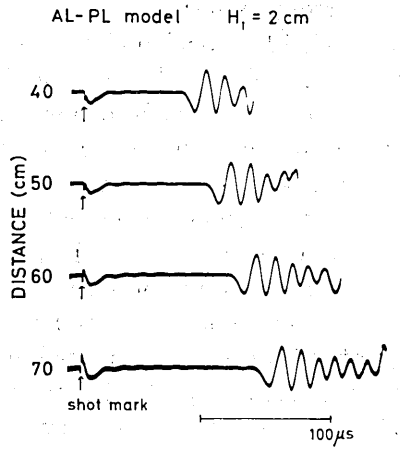

Fig. 9. High gain records for the AL-PL model (H_1=1 cm).

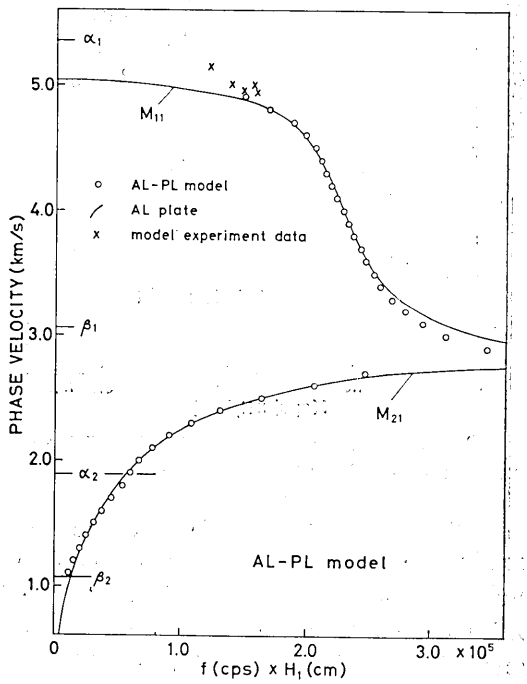

Fig. 10. Dispersion curves for the AL-PL model and for the AL-plate model. Phase velocities for the AL-PL model (open circles) were calculated by the aprroximate methods. Observed dispersion data from wave trains in Fig. 9 are also shown by cross marks.

One interesting question is whether the wave trains similar to the M_{11} wave in the plate model do exist in the present models. Some of the records obtained at a very high gain from a model experiment for the AL-PL model are shown in Fig. 9. The wave trains presented here precede the waves with large amplitude (Fig. 7) and are considered as those similar to the M_{11} wave in the plate model.

Approximate dispersion curves for the AL-PL model were obtained in the region of $\beta_2 < c < \alpha_1$. The results are presented by open circles in Fig. 10. The dispersion curves of the M_{11} and M_{21} waves for the AL-

plate model are also given by solid lines. The resemblance between the two models can be immediately noticed from this figure. Crossmarks in this figure denote the observed phase velocity data from Fig. 9. It was thus ascertained that the wave trains in Fig. 9 were similar to the M_{11} wave in the AL-plate model.

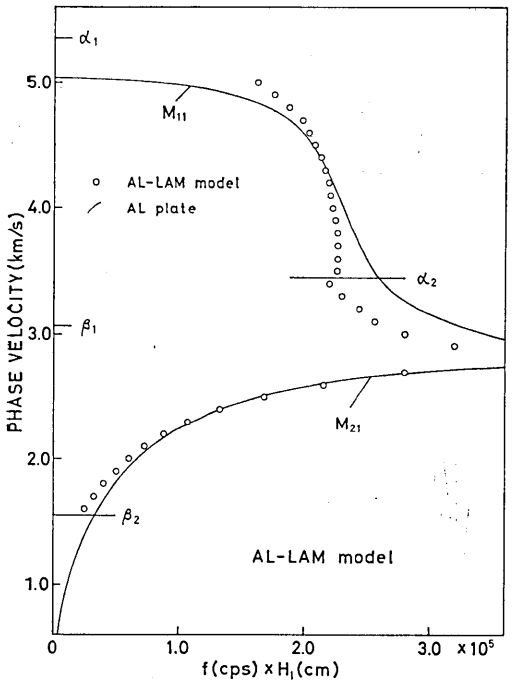

Fig. 11. Dispersion curves for the AL-LAM model and for the AL-plate model.

As shown in Fig. 7, the most predominant wave trains in the AL-PL model are those with $\beta_2 < c < \alpha_2$. In this region, the group velocity curves for the AL-PL model and the AL-plate model should be clearly different from each other because of different gradients of the phase velocity curves.

The leaking mode radiates P wave energy as well as S wave energy into the half space when its phase velocity is greater than α_2. In the vicinity of c equal to α_2, the behaviour of the phase velocity curve is somewhat complicated as shown in Figs. 8 and 10.

The comparison between the dispersion curves for the AL-LAM model and for the AL-plate model is given in Fig. 11. Although the velocity contrast of the AL-LAM model is not so large as that of the AL-PL model, the relation between the dispersive features of this model and of the AL-plate model is still clear.

This resemblance, of course, is expected to be stronger, as the velocity contrast of the model becomes greater. The results in this section do not mean that wave trains in the high-velocity layer model can be analyzed approximately as if they were in the simple plate model. Such an approximation may only be applicable for a model with a very large velocity contrast.

4. Complex root for PAL-models

The elastic wave propagating in a layered half-space is given by the following double integral;

$$u(t, r, z, d)=\int_{-\infty}^{\infty} dk \cdot k \cdot J_0(kr) \int_{-\infty}^{\infty} d\omega \cdot \exp(-i\omega t) \cdot \left[\frac{F(\omega, k, z, d)}{\Delta(\omega, k)}\right], \tag{1}$$

where t, r, z, d denote time, horizontal distance, depth of the receiver and depth of the source, respectively. In the present paper, the contour integral with respect to a complex variable ω is discussed as in Gilbert's (1964) paper. Two sets of branch points, $\omega=\pm\alpha_n k$ and $\omega=\pm\beta_n k$, are located in the complex ω-plane due to two radicals,

$$\nu=(k^2-\omega^2/\alpha_n^2)^{1/2} \quad \text{and} \quad \nu'=(k^2-\omega^2/\beta_n^2)^{1/2}, \tag{2}$$

which are involved in the integral (1). The suffix n is attached to the quantities in the half-space. The resultant four Riemann sheets are labeled as (+, +), (+, −), (−, +) and (−, −) according to the signs of $\mathrm{Re}(\nu)$ and $\mathrm{Re}(\nu')$ [Gilbert (1964)]. Familiar normal mode poles are on the real axis in the (+, +) sheet. When branch lines are fixed along $\mathrm{Re}(\nu)=0$ and $\mathrm{Re}(\nu')=0$, and the (+, +) sheet is chosen as the uppermost one, the integral is evaluated by the sum of branch line contributions and residues of the normal mode poles. If these branch lines are suitably deformed, residues of the complex poles in the uncovered (+, −) and (−, −) sheets are added as a part of the integral [Rosenbaum (1960)]. These new residues yield the concept of the leaking mode. Dispersion curves of the leaking mode can be obtained by tracing the complex roots of the period equation $\Delta(\omega, k)=0$.

The complex roots of the "fundamental mode" for the PAL-models are shown in Fig. 12. In this figure, the abscissa denotes the angular wave number k and the ordinate- the complex frequency

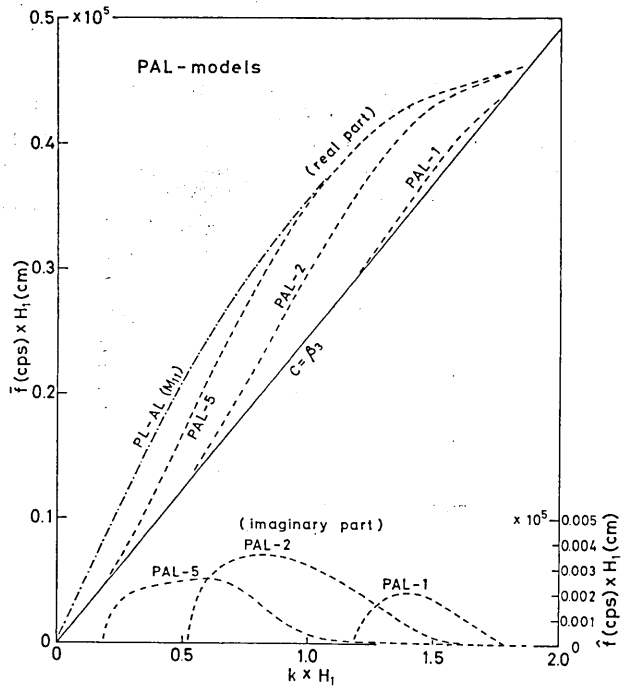

Fig. 12. Complex roots for PAL-models.

$(\bar{f}+i\hat{f})$ respectively. The scale for $\hat{f}$ is largely magnified because it is much smaller than $\bar{f}$. The dispersion curve of the M_{11} wave for the PL-AL model is also presented by a chain line. In the higher frequency range, real parts for PAL-5 and PAL-2 are very close to this curve and imaginary parts are very small. Since the expression of the wave form (1) involves a stationary vibration term, $\exp(-i\omega t)$, the imaginary part of the complex frequency yields the attenuation of the wave train with time. Small imaginary parts correspond to a small attenuation of the wave trains.

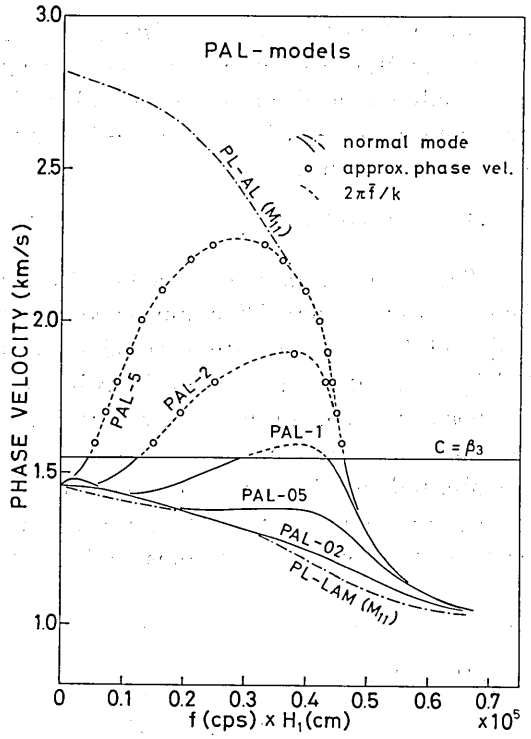

Fig. 13. Comparison of phase velocity curves obtained from complex roots and from approximate solutions for PAL-2 and PAL-5.

The phase velocity curves derived from the real part in Fig. 12 are shown by dashed lines in Fig. 13. Approximate phase velocities for PAL-2 and PAL-5 are given by open circles (See Fig. 2). They agree with the dashed lines very well.

The comparison of the approximate phase velocity with

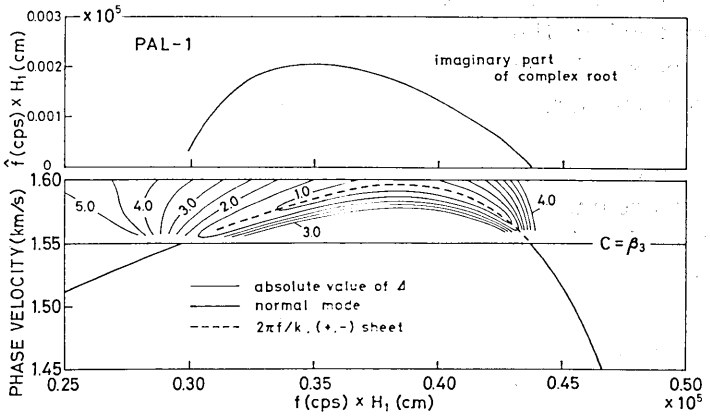

Fig. 14. Comparison of phase velocity curves obtained from complex roots and from approximate solutions for PAL-1.

the complex root for PAL-1 is given in Fig. 14. The absolute value of the period function Δ is drawn by contour lines in $c>\beta_3$ [Yoshii (1969)]. A pronounced "trough" of the contour lines corresponds to the approximate dispersion curve. The phase velocity curve derived from the real part of the complex root (dashed line) is situated just at the centre of this "trough".

5. Complex roots for AL-PL and AL-LAM models

Complex roots for the AL-PL model are given in Figs. 15(a) and (b). The phase velocity curves from the approximate solutions and from the real parts of the complex roots are given in Figs. 16(a) and (b).

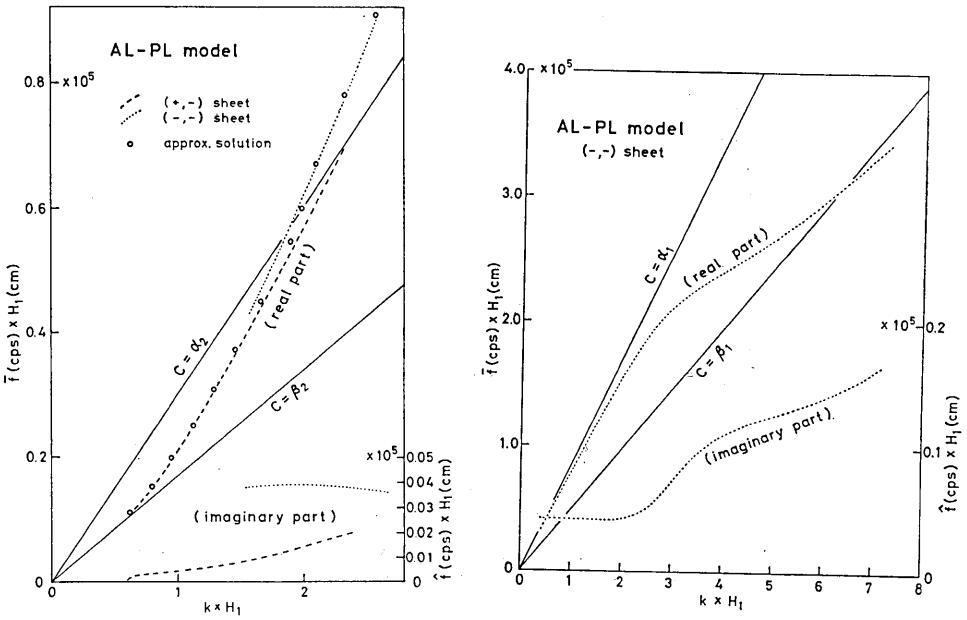

(a) Lower-velocity mode which is simlar to the M_{21} wave in the plate model.

(b) Higher-velocity mode which is similar to the M_{11} wave in the plate model.

Fig. 15. Complex roots for the AL-PL model.

The phase velocity curves obtained in those two ways agree well with each other. The dotted line in Fig. 15(a) shows the complex root in the $(-, -)$ sheet. This root mainly corresponds to the leaking mode whose phase velocity is larger than α_2. The leaking mode of this type may radiate P wave energy as well as S wave energy into the half-space. As shown in Fig. 15(a), this situation is also understood by the larger imaginary part.

As mentioned before, the imaginary part of the complex root yields

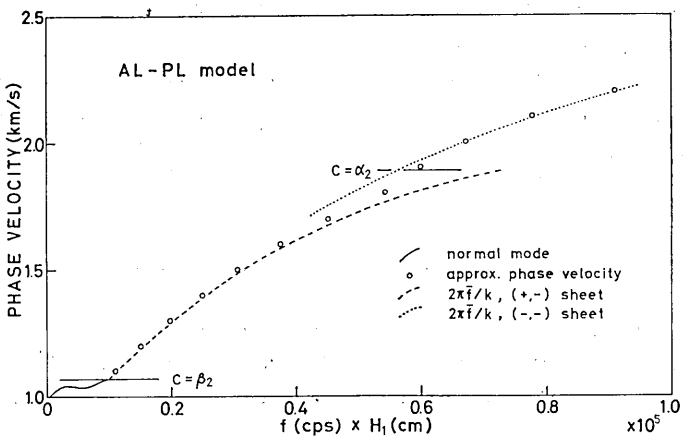

(a) Lower-velocity mode.

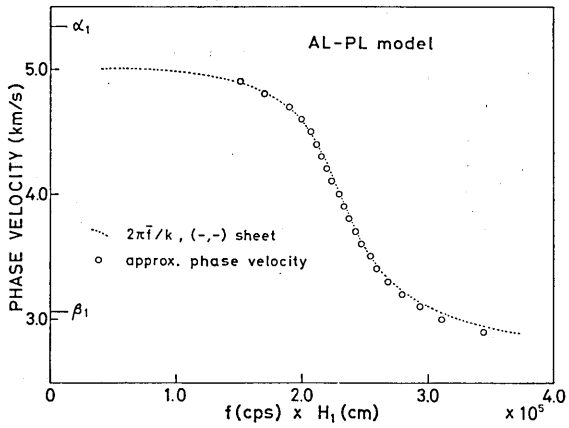

(b) Higher-velocity mode.

Fig. 16. Comparison of dispersion curves obtained from complex roots and from approximate solutions for the AL-PL model.

attenuation of the leaking mode. The relation between the attenuation coefficient α with respect to distance and the imaginary part $\hat{f}$ is

$$\hat{f}=\alpha U/2\pi\,, \tag{3}$$

where U denotes the group velocity. Observed attenuation data from the records in Fig. 7 are given in Fig. 17 [Yoshii and Suzuki (1969)]. Observed data for a model with a layer thickness of 2.0 cm are also given. Since the attenuation discussed here should be zero in the normal mode region, attenuation coefficients were determined from the amplitude spectra all of which were normalized at a point of the normal mode-leaking mode boundary. The results are shown by open circles.

It is noticeable that the obtained attenuation data involve the effect of absorption in the media, but the analytical estimate of the absorption for the leaking mode is now impossible. The absorption in the plastics plate is rather large and is close to $Q=28$. Since this value should correspond to the maximum absorption in the AL-PL model, this effect was subtracted from the observed attenuation data. The results are shown by closed circles in the same figure. Attenuation coefficients due to the energy leakage must exist somewhere between these open and closed circles. The imaginary parts, which have already been represented in Fig. 15(a) are reproduced in Fig. 17. These curves explain the observed attenuation data very well.

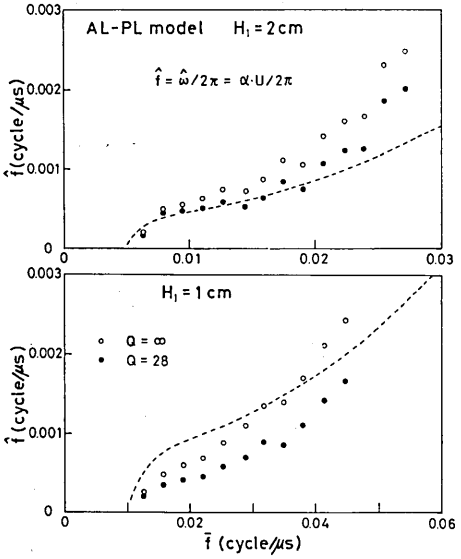

Fig. 17. Comparison of observed attenuation data and the imaginary part of the complex root for the AL-PL model.

As shown in Fig. 15(b), the imaginary part of this mode is rather large except for a range

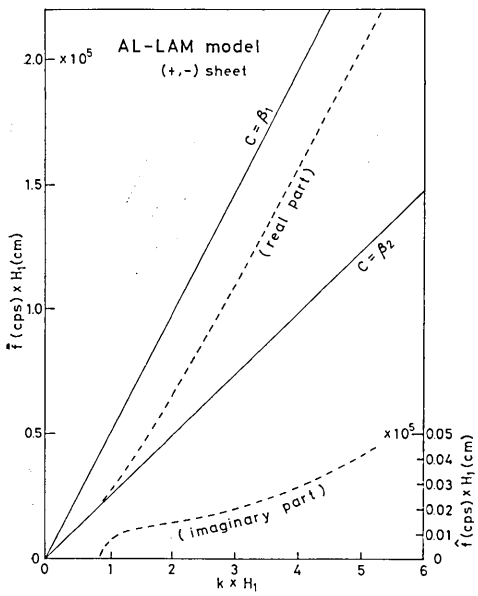

(a) Lower-velocity mode.

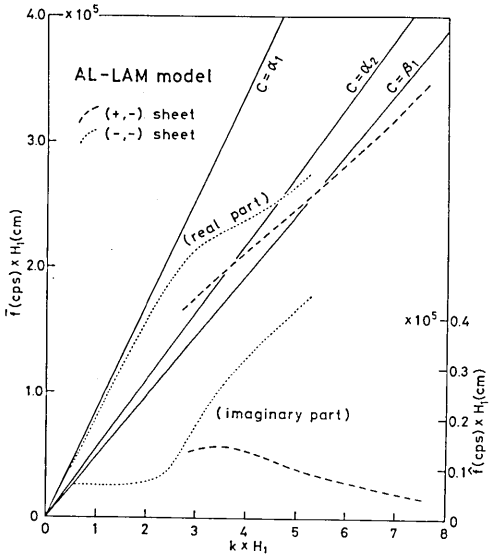

(b) Higher-velocity mode.

Fig. 18. Complex roots for the AL-LAM mode.

of $kH_1<2.5$. It is interesting that actually observed wave trains are restricted in this range (Fig. 10).

Complex roots for the AL-LAM model are shown in Figs. 18(a) and (b). Phase velocity curves derived from the approximate methods and from the complex roots are given in Figs. 19(a) and (b). These figures

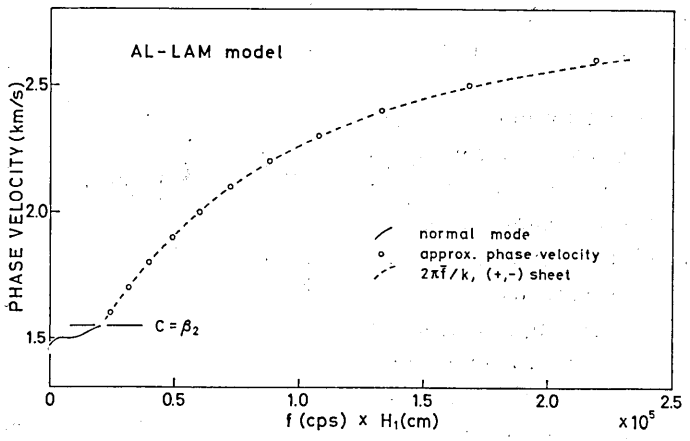

(a) Lower-velocity mode.

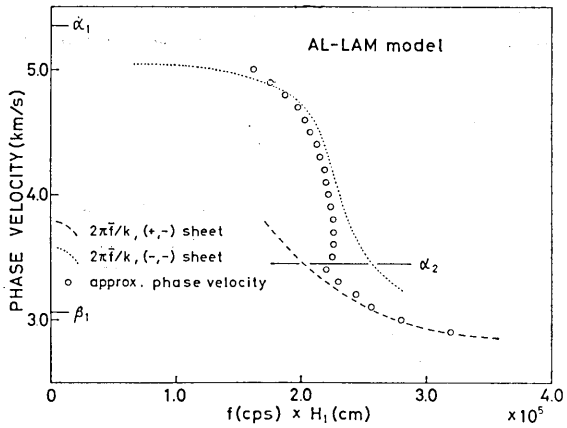

(b) Higher velocity mode.

Fig. 19. Comparison of dispersion curves obtained from complex roots and from approximate solutions for the AL-LAM model.

are essentially similar to those for the AL-PL model, but the complexity due to the position of $c=\alpha_2$ is found in a mode corresponding to the M_{11} wave. Except for a region near $c=\alpha_2$, the agreement between the approximate dispersion curves and dispersion curves from the complex roots is good.

6. Conclusions

The conclusions obtained from the present study are as follows:

1) It is possible to regard a part of, or sometimes the greater part of, the surface wave propagating in the high-velocity layer model, as a kind of leaking mode.
2) Two approximate methods are very effective to obtain dispersion curves of the leaking mode.
3) Dispersion curves for the high-velocity layer models are very unusual; for example, sometimes phase velocity curves show an "inverse dispersion".
4) Observed dispersion data from actual model experiments were well explained by the approximate dispersion curves.
5) The resemblance between dispersive features of the high-velocity layer model and of the so-called plate model is remarkable. The most pronounced wave train in the high-velocity layer model is similar to the M_{21} wave in the plate model.
6) Dispersion curves derived from the real parts of the complex roots agree well with the approximate dispersion curves.
7) Observed attenuation coefficients from an actual model experiment were well explained by the imaginary part of the complex root.

Acknowledgement

The author wish to thank Dr. S. Asano and Dr. K. Tazime for many helpful discussions and suggestions.

This paper is based on a part of a doctorial thesis submitted to the Hokkaido University in March 1970.

References

GILBERT, F., 1964. Propagation of Transient Leaking Modes in a Stratified Elastic Waveguide, *Rev. Geophys.*, **2**, 123-153.

HASKELL, N. A., 1962. Crustal Reflection of Plane P and S Waves, *J. Geophys. Res.*, **67**, 4761-4767.

OLIVER, J. and M. MAJOR, 1960. Leaking Modes and the PL Phase, *Bull. Seism. Soc. Amer.*, **50**, 1-12.

OLIVER, J., F. PRESS and M. EWING, 1954. Two-dimensional Model Seismology, *Geophysics*, **19**, 202-219.

PHINNEY, R. A., 1961. Leaking Modes in the Crustal Wave Guide. Part 1. The Oceanic PL Wave, *J. Geophys. Res.*, **66**, 1445-1469.

PRESS, F. and J. OLIVER, 1955. Model Study of Air-coupled Surface Waves, *J. Acoust. Soc. Amer.*, **27**, 43-46.

ROSENBAUM, J. H., 1960. The Long-Time Response of a Layered Elastic Medium to Ex-

plosion Sound, *J. Geophys. Res.*, **65**, 1577-1613.
SU, S. S. and J. DORMAN, 1965. The Use of Leaking Modes in Seismogram Interpretation and in Studies of Crust-Mantle Structure, *Bull. Seism. Soc. Amer.*, **55**, 989-1021.
TAZIME, K and T. YOSHII, 1969. A Way to Conformal Mapping of the Characteristic Equation of Love-type Wave (4), *Zisin*, **22**, 20-28 (in Japanese).
YOSHII, T., 1969. Characteristics of Some Types of Leaking Modes, *Geophys. Bull. Hokkaido Univ.*, **21**, 117-131 (in Japanese).
YOSHII, T. and K. SUZUKI, 1969. Model Experiments on Surface Waves Propagating in High Velocity Layer Models, *Zisin*, **23**, 236-244 (in Japanese).

37. 高速度層モデルを伝わる表面波の分散

地震研究所 吉 井 敏 尅

表層又は中間層が半無限媒質より速いP波，S波速度を有するようなモデル（以下高速度層モデルと略称する.）を伝わる表面波の性質は，大変興味ぶかい問題である．本論文ではこの種の表面波の性質のうち，主として分散について述べる．

ここであつかわれるモデルは，Table 1 に示すような 3 つの媒質 (plastics, aluminum, Lamiverre) の組み合わせからなるものに限られているが，一般の高速度層モデルの性質についても，今回の結果から容易に推察できることと思う．中間層が高速度である例として，Fig. 1 に示すような 5 つのモデル (3 つの媒質の頭文字をとって PAL-モデルと呼ぶ.)，および表層が高速度である例として AL-LAM および AL-PL モデルが選ばれた．本研究の主要な結論は次のとうりである．

1) 高速度層モデルを伝わる表面波の一部（時には大部分）は一種のリーキングモードと考えられる．
2) このリーキングモードの分散曲線の計算には，Oliver and Major (1960) および Su and Dorman (1964) による近似法が大変有効である．
3) 高速度層モデルの分散曲線は一般に極めて特異な形をしている．例えば，AL-PL および AL-LAM モデルを伝わる表面波の主要部分の位相速度は，“逆分散”で特徴づけられる．PAL-モデルの場合も，一部に“逆分散”をふくむ複雑な形をしている．
4) モデル実験で，AL-LAM および AL-PL モデルを伝わる表面波を観測したところ，その分散は近似法により求められた分散曲線と良く一致した．
5) 位相速度が“逆分散”を示すことからも推察されるように，高速度層モデル（特に表層が高速の場合）は，いわゆる“板”モデルと類似の性質を持つ．この“逆分散”は，板モデルを伝わる M_{21} 波（非対称振動）に対応することは言うまでもない．
6) 近似法とは別に，特性方程式 $\Delta(\omega, k)=0$ の複素根 (ω: 複素数, k: 実数) を計算し，その実数部から位相速度を求めてみると，近似法によるものと一部分をのぞいて極めて良く一致する．この不一致は，位相速度が半無限媒質のP波速度に近い部分に限られている．
7) AL-PL モデルを伝わるリーキングモードの減衰を実際のモデル実験から求めてみると，複素根の虚数部でうまく説明できる．

今回の研究から明らかなように，高速度層モデルを伝わる表面波の解析には，リーキングモードの考えを使うのが最も簡単かつ見事な方法と思われる．